frontiers | Frontiers in Mechanical Engineering

TYPE Original Research
PUBLISHED 25 November 2024
DOI 10.3389/fmech.2024.1488407

OPEN ACCESS

EDITED BY
Balasubramaniam Vengudusamy,
Klüber Lubrication München GmbH & Co. KG, Germany

REVIEWED BY
Seyed Borhan Mousavi,
Texas A and M University, United States
Milan Bukvic,
University of Kragujevac, Serbia

*CORRESPONDENCE
Sougata Roy,
sroy@iastate.edu

RECEIVED 29 August 2024
ACCEPTED 06 November 2024
PUBLISHED 25 November 2024

CITATION
Bhowmik P, Sharma BK, Sarker MI, Mainali K, Wang Y, Tang C and Roy S (2024) Exploring the additive compatibility and tribological behavior of regular and high oleic soybean oil.
Front. Mech. Eng. 10:1488407.
doi: 10.3389/fmech.2024.1488407

Exploring the additive compatibility and tribological behavior of regular and high oleic soybean oil

Piash Bhowmik[1], Brajendra K. Sharma[2], Majher I. Sarker[2], Kalidas Mainali[2], Yachao Wang[1], Clement Tang[1] and Sougata Roy[3]*

[1]Department of Mechanical Engineering, University of North Dakota, Grand Forks, ND, United States, [2]US Department of Agriculture, Agricultural Research Service Eastern Regional Research Center, Sustainable Biofuels and Coproducts Research, Wyndmoor, PA, United States, [3]Department of Mechanical Engineering, Iowa State University, Ames, IA, United States

As the demand for biobased lubricating oils continues to rise, there is a growing focus on exploring diverse oil types. Particularly noteworthy is the surge in demand for high oleic oils, which offer enhanced stability, and a richer oleic acid content compared to their regular oil counterparts. However, the performance of high oleic soybean oil (HOSO) with additives compared to regular soybean oil (RSO), remains unclear. This study is focused on revealing the compatibility of both regular soybean oil (RSO) and high oleic soybean oil (HOSO) with select antiwear and antioxidant additives, specifically zinc dialkyl dithiophosphate (ZDDP), and zinc dialkyl dithiocarbamate (ZDDC) combined with antimony dialkyldithiocarbamate (ADDC), along with a comparative performance analysis of these additives. Reciprocating friction, wear, and electrical contact resistance-based analyses were conducted to evaluate additive compatibility and wear mechanisms at room temperature lubrication conditions. Interestingly, it was observed that for the select additives, the compatibility with regular soybean oil (RSO) was better than that of high oleic soybean oil (HOSO). RSO with additives showed around 28% reduction of wear volume whereas, it was only 8% for HOSO with additives. Additional physiochemical property analyses were conducted on the lubricants to correlate the observed tribological behavior. The worn-out surfaces of the test samples were characterized thoroughly to reveal the dominant wear mechanisms.

KEYWORDS

soybean oils, biolubricant, lubricant additives, wear mechanisms, tribology

1 Introduction

The role of lubricating oils is crucial in keeping various industries running smoothly, including automotive, manufacturing, aerospace, and energy production. Lubricating oils are essential in machines as they prevent wear and tear by creating a protective layer between moving parts (Qin et al., 2019). Mineral oil-based lubricants find extensive use in many industries due to their excellent lubrication qualities, easy availability, and chemical stability. Even electric vehicles, despite running on batteries, rely on lubricating oil for certain components. In recent times, there has been a growing concern for finding

alternatives to petroleum oils. This is primarily due to their non-renewable nature, toxicity, and lack of biodegradability (Shodji Tamada et al., 2012), (Vazquez-Duhalt, 1989). According to recent studies, around 50% of the lubricants used globally end up polluting the environment due to several reasons like their usage, accidental leaks, evaporation, or improper disposal techniques (Reeves et al., 2017). Mineral oils are exhaustible resources, and their continuous usage is contributing to their depletion. Global initiatives are being carried out to reduce the usage of petroleum-based oils due to the adverse effects they have on the environment.

It is evident that the world is gradually shifting towards renewable energy and materials sources, and the lubrication industry is no exception. In recent times, there has been a surge in research investigations to explore the tribological behavior of biobased oils. These oils are extracted from natural sources such as coconut (Jayadas et al., 2007), (Jayadas and Nair, 2006), rapeseed (Ruggiero et al., 2017), (Ravasio et al., 2002), jatropha (Ruggiero et al., 2017), castor (Ouyang et al., 2021), canola (Reeves and Menezes, 2017), avocado (Reeves and Menezes, 2017), soybean (Adhvaryu and Erhan, 2002), (Cheenkachorn, 2013), sunflower (Fox et al., 2004), (Kumar and Gautam, 2022), and palm oil (Masjuki et al., 1999), (Shomchoam and Yoosuk, 2014). An alternative option that presents a significant opportunity to repurpose discarded waste is the use of waste cooking oil as a lubricating oil. This approach can serve as a viable solution to reduce reliance on petroleum-based oils and minimize their environmental impact (Milano et al., 2022). Soybean oil is one of the most widely produced biobased oils across the world (Wilson, 1998). It has been extensively researched in the area of biobased lubricating oil, where different types of soybean oils such as regular soybean oil, chemically modified soybean oil like high oleic, epoxidized, isopropylation or thermally modified soybean oils have been used (Adhvaryu and Erhan, 2002), (Napolitano et al., 2018), (Bhowmik et al., 2024), (Adhvaryu et al., 2004). Researchers have conducted studies to examine the efficacy of these oils in high-temperature lubricant applications as well.

Hwang et al. (Hwang and Erhan, 2006) performed a chemical alteration on epoxidized soybean oil (SBO) using different alcohols and sulfuric acid as a catalyst. This reaction resulted in products where the epoxide rings were opened. This product was subjected to a series of reactions involving alcohols and sulfuric acid as a catalyst. This was followed by esterification with acetic anhydride and pyridine. The process resulted in final products that demonstrated enhanced resistance to oxidation and had low pour points. Bhowmik et al. (Bhowmik et al., 2024) studied the tribological behavior and physicochemical properties of chemically modified high oleic soybean oil (HOSO) using isopropylation approach at different operating temperatures. They observed an improvement of 10.6% reduction in wear volume due to the select chemical modification process as compared to that of regular HOSO. Esterification forms esters from acids and alcohols, enhancing the oil's properties. Transesterification converts triglycerides into fatty acid methyl esters (FAME), improving lubrication (McNutt and He, 2016). Estolides, formed from fatty acids, also boost oil performance. The production of estolides, cyclic esters, improves the viscosity and stability of oils, making them more suitable for lubrication. Acetylation adds acetyl groups to improve thermal stability and lubricating properties (Cermak et al., 2017). Genetic modification techniques, such as CRISPR-Cas9, enable precise edits to oilseed crops, boosting oil yield and fatty acid composition for better lubrication. Traditional transgenic approaches modify metabolic pathways by inserting foreign genes, further enhancing oil properties for lubrication (Hamnas and Unnikrishnan, 2023).

Lubricant properties are improved through the modification of oils, particularly vegetable oils, which are prone to oxidation because of double bonds. Bis-allylic protons adjacent to these double bonds are the primary reason for the radical attacks and oxidation process in biobased oils (Fang and Mccormick, 2006), (Adhvaryu et al., 2005), (Kumar, 2017). The oxidation process comprises of three primary stages, namely, initiation, propagation, and termination. During the initiation stage of the lubricant oxidation process, the components of the lubricant react with one or more catalysts, resulting in the formation of free radicals - highly reactive molecules that combine with other molecules to create new chemical compounds. In the propagation stage of the oxidation process, various types of free radicals and catalysts react with each other in intricate ways, resulting in the generation of additional free radicals and oxygenated compounds. The termination stage signifies the conclusion of the oxidation process, which can have either a positive or negative outcome (Fox and Stachowiak, 2007). To enhance their performance, additives such as nano particle antioxidants, antiwear agents, and friction modifiers are mixed with the oils.

Mousavi et el (Mousavi and Zeinali Heris, 2020). studied the effects of zinc oxide (ZnO) nanoparticles on diesel oil's thermophysical and tribological properties. The addition of ZnO reduced the coefficient of friction by 5.86% and decreased pin mass loss by 86% compared to pure diesel oil, showing significant improvements in anti-wear performance. In another study the same research group enhanced the tribological properties of synthetic biodegradable PAO oil using a combination of nanoparticles. Copper (Cu) nanoparticles reduced friction and wear, titanium dioxide (TiO_2) improved stability, manganese dioxide (MnO_2) enhanced tribological characteristics, and graphene oxide (GO) was used for better nanoparticle dispersion. The Cu/TiO_2/MnO_2-doped GO nanocomposite resulted in a significant improvement, with a maximum anti-wear feature of around 46% (Mousavi et al., 2024). In other studies, it has been observed that ZnO and MoS_2 nanoparticles can effectively improve the tribological properties of biobased oils and also diesel oil, enhancing their friction-reducing and anti-wear performance (Mousavi et al., 2021), (Mousavi et al., 2020), (Mousavi et al., 2019). Antioxidant additives prevent oxidation caused by high temperatures and oxygen exposure, while antiwear additives reduce friction and wear on metal surfaces, enhancing equipment longevity. In addition to these, friction modifiers, nanoparticles, or ionic liquids may also be used to enhance their friction and wear behavior in different application domains (Roy et al., 2019), (Roy et al., 2021). Researchers investigated the effects of adding copper oxide nanoparticles (CuO) to Sal oil after chemically modifying it through the epoxidation process. They added CuO nanoparticles in varying concentrations and dispersed them properly through an ultrasonication process. Minimum COF was observed when the concentration of nanoparticles in the modified oil was 0.5%, which resulted in an 8% reduction in friction compared to the raw oil.

TABLE 1 Fatty acids percentages in RSO and HOSO captured using GC-MS.

	Palmitic acid	Stearic acid	Oleic acid	Linoleic acid	Linolenic acid
RSO	10.9%	3.4%	22.6%	56.4%	6.5%
HOSO	4.7%	2.3%	89.3%	3.8%	---

Furthermore, adding CuO nanoparticles up to 0.5% also minimized the wear of the pin in comparison to using raw Sal oil, reducing wear by approximately 4.2% (Kumar Chaurasia et al., 2020). According to recent research, lubrication behavior of soybean oil can be enhanced significantly by incorporating zinc dialkyl dithiophosphate (ZDDP) as lubricant additive. The addition of ZDDP has been found to enhance wear resistance of soybean oil by up to 57% compared to its regular version. It is also possible to further boost the performance of soybean oil by combining it with other antiwear agents available commercially (Bahari et al., 2018). Sharma et al. (Sharma et al., 2007) found that the zinc dialkyl dithiocarbamate (ZDDC) antioxidant performed better compared to diphenylamine and hindered phenol while additized with vegetable oils to develop eco-friendly lubricants. Furthermore, the researchers observed that incorporating antimony dialkyldithiocarbamate (ADDC) to diphenylamine improved its inhibition capabilities (Sharma et al., 2007).

Despite the extensive research and development efforts focused on using soybean oil as a lubricating oil, there is currently no focused investigation available exploring the compatibility of major antiwear and/or antioxidative additives on tribological behavior of two major types of soybean oils specifically regular and high oleic versions. In this study, a 1% (w/w) concentration of ZDDP was mixed with both regular soybean oil (RSO) and high oleic soybean oil (HOSO). Simultaneously, a 2% (w/w) ZDDC and a 2% (w/w) concentration of ADDC were blended with both oils. The study aimed to assess the compatibility of these additives and their impact on the physicochemical and tribological properties of both types of soybean oils. Overall, the major focus was to identify the most effective additive for soybean oil among those tested in this investigation and the additized RSO and HOSO helps in wear resistance under controlled tribological experiments in room temperature.

2 Methodology

2.1 Materials

The regular soybean oil (RSO) and high oleic soybean oil (HOSO) used for this research were purchased from CHS Inc. (Minnesota, USA). The amount of lubricant used in each test was 8 mL. HOSO was chosen for this experiment because it has been researched extensively for its stability as it contains tocopherol (Napolitano et al., 2018). Tocopherol serves as an antioxidant that aids in preventing oxidative damage by scavenging free radicals (Seppanen et al., 2010). Analyses of these oils were performed using Gas Chromatography-Mass Spectrometry (GC-MS), and the findings are shown in Table 1. HOSO is rich in monounsaturated fatty acids, especially oleic acid (89.3%), while RSO is abundant in polyunsaturated fatty acids, specifically linoleic acid (56.4%). AISI 52100 is being used as bearing material because of its exceptional hardness, wear resistance and durability (Bhadeshia, 2012). 6 mm diameter AISI 52100 steel balls as counter material against AISI 52100 steel flats in this study. Vanderbilt Chemicals, USA provided the Antioxidant additive zinc dialkyl dithiocarbamate (ZDDC) and antiwear additive antimony dialkyldithiocarbamate (ADDC). Zinc dialkyl dithiophosphate (ZDDP) was obtained from Luoyang Tongrun Nano Technology Co. Ltd, China.

2.2 Preparation of lubricants

In this experiment, RSO and HOSO were used as base oils. Zinc dialkyl dithiophosphate (ZDDP) was mixed with both RSO and HOSO at concentrations varying from 0.5% to 2% (w/w), with a step size of 0.5%, a range chosen based on previous studies. To prepare the oil-ZDDP blend, the mixture was first stirred in a magnetic stirrer at 60°C for 5 min. This was followed by 30 min of stirring at room temperature. Subsequently, the mixture underwent ultrasonic sonication at a frequency of 40 kHz for 1 h at room temperature. The results indicated that the 1% (w/w) ZDDP concentration yielded the best performance in terms of tribological behavior and lubricant stability. Zinc dialkyl dithiocarbamate (ZDDC) was mixed with RSO and HOSO at concentrations ranging from 0.5% (w/w) to 2% (w/w), with a step size of 0.5%. Initially, the oil-ZDDC mixture was stirred for 30 min at room temperature and then subjected to ultrasonic sonication for 1 h to improve dispersion. From tribological behavior and stability viewpoint, 2% (w/w) ZDDC concentration was found optimized content for soybean oils. Following this, a mixture of 2% (w/w) ZDDC and the base oil was prepared, and antiwear additive antimony dialkyldithiocarbamate (ADDC) was incorporated at concentrations ranging from 0.5% (w/w) to 2% (w/w), with an increment of 0.5% using the same procedure. The results led to the selection of a 2% (w/w) ZDDC and 2% (w/w) ADDC mixture due to its superior performance.

2.3 Pressure differential scanning calorimetry (PDSC)

The stability of oxidation was evaluated using a PDSC (Q20) tool manufactured by TA Instruments, based in New Castle, DE, USA. To conduct the experiment, a pinhole hermetically sealed aluminum pan was used to hold 2 µL of the sample. The sample was then subjected to oxidation by heating it at a ramp rate of 10 °C/min. The oxidation process was carried out in the presence of air at a pressure of 1,378.95 kPa (200 psi). The initial temperature at which the oxidation process starts, also known as onset temperature (OT), was determined by drawing a tangent on the steepest slope of the reaction exotherm. A higher OT indicates greater oxidative stability of the vegetable oil. The PDSC technique used a small

sample size (microgram) and was conducted in triplicate. The reported values are the average of three measurements. In earlier studies (Sharma et al., 2009) it was demonstrated that the oxidative stability data obtained through PDSC was comparatively more consistent than the oxidative stability index (OSI) measured using the Rancimat method EN 14112. The PDSC onset temperature was also shown to have a good correlation with Rancimat OSI values (R^2 value of 0.91). The PDSC method offered a notable advantage over other methods in that it can effectively measure the oxidative stability of both low and high oxidation-prone oils, regardless of whether they were additized or unadditized.

2.4 Thermogravimetric studies

A thermogravimetric analysis was carried out to investigate the thermal behavior of the samples by subjecting them to different heating rates under an air environment. The TA Q500 V20.13 Build 39 instrument was used to conduct thermogravimetric analysis. The samples, with a mass range of 10–15 mg, were analyzed by applying different heating rates (5, 10, 15, and 20 °C/min) until the final temperature of 800°C was reached. The weights of all samples were maintained at 10 mg in order to reduce the disparity between heat and mass transfer. To ensure the accuracy of the results, all tests were carried out in duplicates, as per the methodology outlined in the literature (Kruka et al., 1995).

2.4.1 Kinetic analysis

The "Friedman method," which is an isoconversional technique, was utilized to analyze the samples. The relationship between the activation energy rate and the conversion rate of the samples was established using a modified Arrhenius equation, which is expressed as follows (Equation 1.1) (Roy et al., 2019):

$$\frac{da}{dt} = Ae^{-\frac{E}{RT}} f(a) \tag{1.1}$$

The symbol α represents the dimensionless conversion degree, while t denotes time (s). The frequency factor A is expressed in units of s^{-1}, and E corresponds to the activation energy (J mol^{-1}). The absolute temperature is represented by T in Kelvin, while R is the universal gas constant with a value of 8.3145 J K^{-1} mol^{-1}. Finally, the differential conversion function is denoted by f(α) (Kruka et al., 1995). Under non-isothermal conditions, where a constant heating rate is applied (Equation 1.2), Equation 1.1 can be expressed as follows (Zhang et al., 2023).

$$\frac{da}{dt} = \frac{A}{\beta} Ae^{-\frac{E}{RT}} f(a) \tag{1.2}$$

By taking the natural logarithm of both sides of the previous equation, the resulting expression is as follows (Equation 1.3):

$$ln\left(\frac{d\alpha}{dt}\right) = ln\left[\beta\left(\frac{d\alpha}{dt}\right)\right] = ln[Af(\alpha)] - \frac{-E_a}{RT} \tag{1.3}$$

Assuming that the conversion function f (α) stays constant for a constant amount of α, lubricant deterioration under this scenario (iso-conversion) is only dependent on temperature. For constant values, a plot of ln [dα/dt] vs. 1/T should show a straight line, the slope of which is equal to $-E_a/R$. Determining the reaction process is challenging since the complex reaction frequently comprises several chemical and diffusion phases. Iso-conversion techniques, which enable the estimation of kinetics parameters like activation energy (E_a) and pre-exponential factor (A), form the basis of the kinetics of free models. Activation energy is the energy threshold that must be overcome by the reactants to initiate and sustain a specific chemical reaction. The number of collisions that happen in a certain amount of time is known as the pre-exponential factor.

2.5 Analysis of viscosity, viscosity index, and density

To determine the dynamic viscosity and densities of biobased oils, an SVM3001/G2 viscometer was used along with an Xsample 530 Automatic Sample Changer from Anton Paar GmbH, Graz, Austria. The measurements were taken at 40°C and 100°C, respectively, following ASTM D7042 ("Standard Test Method for Dynamic) and ASTM D4052 ("Standard Test Method for Density). 20 mL of each sample was transferred into a vial and placed in the automated sample changer's carousel. The device measured the dynamic viscosity and density values at 40°C and 100°C respectively, to automatically present the kinematic viscosity at these temperatures. Additionally, the ASTM D2270 ("Standard Practice for Calculating Viscosity) standard was followed to determine the viscosity index (VI) of biobased oils by utilizing the kinematic viscosity data at 40°C and 100°C, which was also determined automatically. SVM3001 smart viscometer measures several parameters of a sample such as kinematic and dynamic viscosity (ASTM D7042), viscosity index (ASTM D2270), density (ASTM D4052), and API grades (API 2540) automatically using a density cell and a viscosity cell in the temperature range of −20°C–135°C with internal Peltier control and no external thermostat. It measures kinematic/dynamic viscosity in the range of 0.2–30,000 mPa s and density (0.60–3 g/cm3) on a small amount of sample as little as 2 mL.

2.6 Cloud point (CP)

The cloud point was assessed following ASTM D5773 ("Standard Test Method for Cloud) guidelines with a Phase Technology PCA-70Xi automated instrument designed for cloud/pour point analysis. Phase analyzer instrument PCA-70Xi (Phase Technology) measures pour and cloud points as per ASTM D5949 and D5773 respectively with sample as small as 0.15 mL and sample temperature range of −88°C–70°C. Before testing, the samples were kept in the lab at a stable room temperature of 22°C ± 1°C. Next, a precise volume of 0.150 ± 0.005 mL of the sample was placed into a sealed chamber with a reflective bottom surface within the instrument. The sealed chamber underwent a vacuum process to eliminate surrounding moisture. Following this, the samples were gradually cooled at a consistent rate of 1.5°C ± 0.1°C per minute. An internal light source within the chamber consistently illuminated the sample from an angle, while an optical detector positioned directly above the sample continuously monitored its condition. As the

sample was in its liquid state, the light passed through it, reflecting off the chamber's bottom. When the sample cooled and crystals started forming, they caused the directed light to scatter, with some of it directed towards the optical sensor positioned directly above the sample. To determine the cloud point, the temperature at which crystals began to form in the sample was identified. This was accomplished by measuring the temperature of the sample at which directed light was deflected onto the optical sensor. The effective temperature range determined for this method spanned from −60°C to 49°C.

2.7 Pour point (PP)

The pour point analysis (ASTM D5949 ("Standard Test Method for Pour)) followed the determination of the cloud point without delay. The optical sensor detected a noticeable change in optical scattering when the sample was exposed to a burst of dry air. The sample underwent cooling at a consistent rate of 1.5°C per minute while pulses of dry air were introduced at intervals of every 3°C. Upon freezing the sample, there was no observable shift in the optical response. To determine the pour point, the reading just prior to this action was identified. For instance, if no optical shift was detected at −27°C when the dry air was applied, the pour point would be recorded as −24°C. This method's effective range was established between −57°C and 51°C.

2.8 Reciprocating friction and wear tests

Friction and wear characteristics were evaluated through tests performed on a reciprocating ball-on-flat tribometer. These tests were conducted using a Rtec tribometer (MFT 2000), manufactured by Rtec Instruments, based in the United States. The electrical contact resistance (ECR) between the ball and the flat was measured with this instrument. Using the ECR measurement can provide strong evidence that an insulating tribofilm has formed on the contact surfaces. For this study, AISI 52100 steel was employed as the flat and balls (6 mm diameter) of the same material used as the counter material. To ensure precision, the flat samples were polished until they attained an average surface roughness (Ra) of below 0.1 µm. Surface roughness analysis was conducted using a Profilm 3D white light profilometer sourced from KLA Instruments, USA. The experiments involved the application of a force of 75N, which led to a maximum Hertzian contact pressure of 2.78 GPa. The tribotests were performed at room temperature, where the sliding velocity and total sliding distance were set to 0.1 m/s and 500m, respectively. In order to ensure the accuracy of the test results, each experiment was conducted three times and corresponding data was captured. A schematic diagram of the testing setup with complete details of the lubricant, sample holder and wiring setup of electrical contact resistance (ECR) is depicted in Figure 1. Following the experiments, wear volume and wear depth for each sample were analyzed using the Profilm 3d white light interferometer. Scanning electron microscopy (SEM) and energy-dispersive X-ray spectroscopy (EDS) was utilized to analyze the major wear mechanisms. SEM imaging was performed with the Quanta FEG 650 model from FEI Inc., USA, while EDS analysis was conducted using the Bruker Nano XFlash SUE six system equipped with Bruker Quantax software manufactured by Bruker Inc., USA.

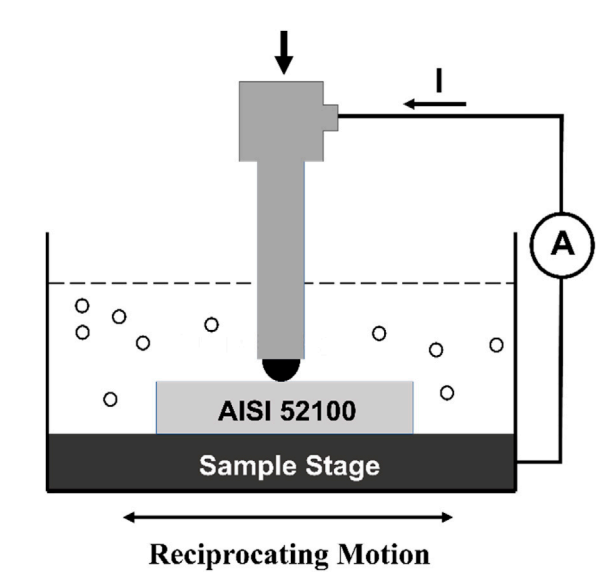

FIGURE 1
Schematic diagram of the tribology testing apparatus.

3 Physicochemical properties of the vegetable oils

3.1 Density

The density of the test lubricants displayed in Table 2 confirms that both RSO and HOSO oils had similar values. This is anticipated, as both RSO and HOSO have comparable proportions of total unsaturated fatty acid chains, 85.5% (oleic, linoleic, and linolenic acids) and 93.1% (oleic and linoleic acids), respectively. The density of natural triglycerides mostly relies on the compactness of their fatty acid chains; linear-saturated chains provide superior compactness compared to unsaturated chains. Additives did not change the density levels significantly. With an increase in temperature, the density of all oils decreased. This is because the molecules in the substance gain kinetic energy and begin to move more rapidly, causing expansion. The increase in volume that occurs due to this expansion leads to a decrease in density (Sahasrabudhe et al., 2017). Density changes were observed with variations in temperature; however, at a specific temperature, all samples exhibited comparable density numbers.

3.2 Kinematic viscosity and viscosity index

The ability of a fluid to prevent internal flow when gravitational forces are acting on it is known as kinematic viscosity. The viscosity index (VI) is a number that shows how the thickness of a fluid changes as the temperature changes. A high VI indicates that the viscosity of a fluid is less prone to change over a broad temperature range. This makes the fluid more stable in a wider temperature

TABLE 2 Physicochemical properties of the base oils additive mixtures.

	Temperature (°C)	RSO	HOSO	RSO + ZDDP	HOSO + ZDDP	RSO + ADDC + ZDDC	HOSO + ADDC + ZDDC
Density(g/cm3)	40	0.9066	0.8993	0.9081	0.90065	0.91005	0.90295
	100	0.8668	0.8596	0.8682	0.8609	0.87015	0.8632
Kinematic Viscosity (mm2/s)	40	30.69	38.93	30.561	38.8425	31.3485	39.6625
	100	7.53	8.49	7.4808	8.4357	7.50625	8.45505
Dynamic Viscosity (mPa/s)	40	27.83	35.02	27.7515	34.9835	28.528	35.813
	100	6.53	7.30	6.4946	7.26245	6.53155	7.29855
Viscosity Index		228.3	203.6	227.095	202.325	220.72	197.66
Pour Point (PP, °C)		−15	−15	−18.0	−18.0	−15.0	−21.0
Cloud Point (CP. °C)		−8.1	−10.9	−6.3	−7.1	−7.3	−9.1

[a]Every attribute value is an average calculated using three different measurements.

range. The comparison of kinematic viscosity and viscosity index (VI) for RSO, HOSO, and the additives blended with these oils are demonstrated in Table 2. Based on the data presented in Table 2, The viscosity of HOSO was significantly higher than that of RSO. Specifically, at a temperature of 40°C, the viscosity of HOSO is 26% higher than that of RSO, and at a temperature of 100°C, it is 12% higher. This can be attributed to the higher percentage of oleic acid in HOSO. It is evident from Table 1 that RSO has a considerably greater proportion of linoleic acid (56.4%) than HOSO (3.8%). Linoleic acid is a type of polyunsaturated fatty acid, while HOSO contains a higher percentage (89.3%) of oleic acid, which is a type of monounsaturated fatty acid. It is worth noting that polyunsaturated fatty acids have more double bonds than monounsaturated fatty acids. When a molecule has a higher number of double bonds, it tends to have a lower viscosity (Giakoumis and Sarakatsanis, 2018). When it comes to the molecular structure of oils, longer chains tend to lead to stronger intermolecular interactions, particularly Van der Waals forces, between neighboring molecules. These interactions can hinder the movement of the molecules and ultimately contribute to higher viscosity. Ramirez-Verduzco et al. had established a correlation between the number of double bonds and viscosity (Ramírez-Verduzco et al., 2012). This phenomenon was also noted in a separate study where high oleic soybean oil exhibited a higher viscosity value (Okafor and Nwoguh, 2020). It can be observed that the additives used in the experiment do not have a significant influence on the viscosity. However, at a temperature of 40°C, a slight increase in viscosity can be seen when RSO and HOSO were blended with ZDDC and ADDC. Nevertheless, the increase in viscosity is minimal. At 100°C, no change was observed. All oils had a decreasing kinematic viscosity as the temperature rose. With an increase in temperature, the kinetic energy of fluid molecules also increased, leading to more rapid movement and frequent collisions with each other. These increased molecular collisions disrupt the intermolecular forces that contribute to viscosity, making it easier for the fluid to flow. Additionally, at higher temperatures, the fluid molecules have more thermal energy, which can overcome the attractive forces between them, further reducing viscosity (Sahasrabudhe et al., 2017). According to the findings presented in Table 2, it could be observed that RSO and RSO with additives had a higher viscosity index value than HOSO and HOSO with additives. Due to its low viscosity index, HOSO tended to experience significant variations in viscosity with temperature changes. On the other hand, RSO's viscosity was more likely to remain stable even with temperature fluctuations.

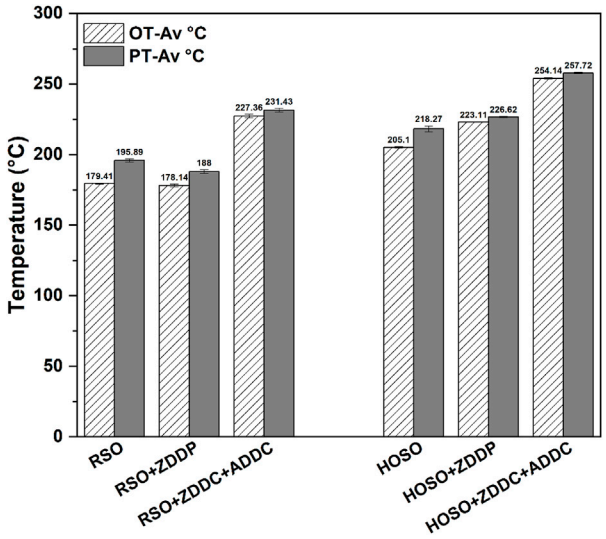

FIGURE 2
Oxidative stability temperatures of the base oils additive mixtures.

3.3 Oxidative stability

Oxidative stability data are presented in Figure 2. The onset temperatures, a measure of oxidative stability, were higher in lubricant samples formulated using high oleic soybean oil (HOSO) compared to regular soybean oil (RSO). HOSO demonstrated greater oxidative stability attributed to its lower unsaturation levels in comparison to RSO (Hong et al., 2014). Between the two additives used, the combination of ZDDC +

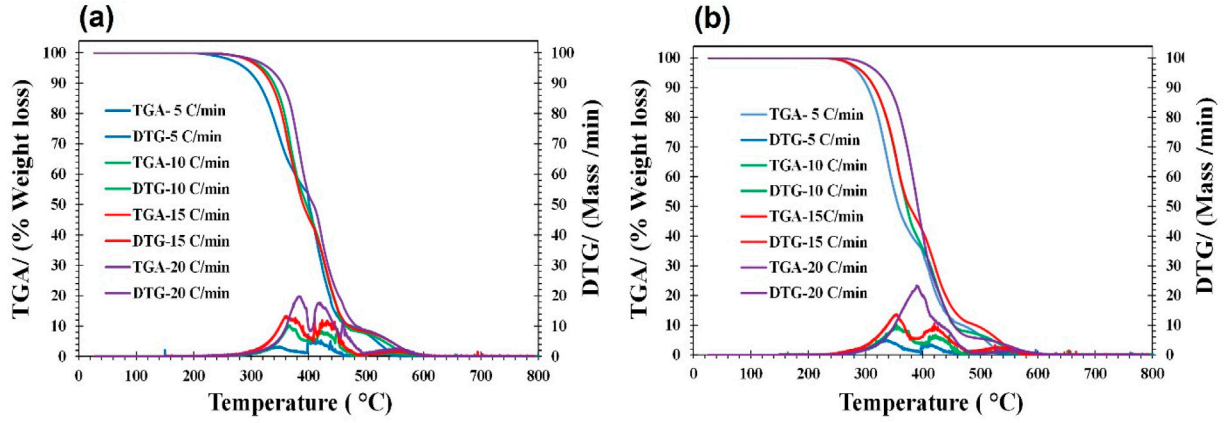

FIGURE 3
TG, DTG curves of vegetable oil **(A)** RSO **(B)** HOSO.

ADDC provided a much higher oxidative stability compared to the samples containing ZDDP additive, by increasing oxidative stability in RSO by about 47°C and in HOSO by about 50°C. The additive combination ZDDC + ADDC was shown to increase the oxidative stability by 50°C over the unadditized versions. The fundamental working mechanisms in enhancing oxidation behavior in case of ZDDP + ADDC case were explained in an earlier publication (Sharma et al., 2007). Based on our earlier work (Sharma et al., 2007),we found that ZDDC + ADDC provides better antioxidant efficiency and strong synergism than ZDDP potentially due to presence of sulfur in metal dithiocarbamates, recycling mechanism for partial recovery of ZDDC or ADDC, and metal ions present in dithiocarbamates. Unadditized HOSO has higher oxidative stability by about 25°C over the unadditized RSO, but this difference increased with the addition of an additive combination of ZDDP to 45°C. HOSO was more responsive to the addition of these additives to increase oxidative stability. A lubricant formulated using HOSO and an additive combination of ZDDC + ADDC provided the highest oxidative stability as seen in Figure 2 from their highest OT and PT. The OT measurement had a maximum standard deviation of 1.2°C, while the standard deviation for peak temperature (PT) was below 2.1°C.

3.4 Thermal degradation under air atmosphere

Thermogravimetric analysis (TGA/DTG) determines a sample's mass change rate in relation to temperature or time in a controlled setting. The measurements are mostly used to ascertain the compositional qualities and thermal and oxidative stabilities of materials. TGA curves represent mass loss below 150°C, Ignition temperature, peak temperature, and residual weight at 800°C. Additionally, the district valley observed in the DTG curves in synthesized lubricants may be attributed to oxidative degradation followed by complete devolatilization combustion. As compared to original samples a) RSO and b) HOSO, the synthesized bio-lubricants showed (As shown in DTG curves under different heating rates) oxidative stability which was related to changes like the chemical structure of esters.

The thermal behavior of the additized products along with parent compounds is shown in Figures 3, 4. For the kinetic analysis, the temperature was maintained at a constant 150°C, and data was normalized. In all samples, the temperature range 300°C–500°C corresponded to oxidative degradation. In most of the samples, complete degradation with no additional loss of mass was observed before 600°C. In each, the mass rate (DTG profiles) indicates the reactivity of the vegetable oils and modified products.

3.5 Activation energy and kinetic analysis

The kinetics of biobased lubricants with different additives was studied in the presence of air. The activation energy and pre-exponential factor of formulated blends were determined using Friedman's differential iso-conversational approach. From TGA profiles, the kinetic parameters of each synthesized product were calculated using a linear variant of the Arrhenius equation concerning conversion (α). In fact, conversions between 0.1 and 0.7 were considered for this study. In all synthesized products, the thermal decomposition process constitutes multistage reactions with respect to conversion levels. In all the cases, the parallel reaction happened from α = 0.05 to α = 0.5 and changed activation energy significantly. This variation in activation energy is due to the devolatilization stage in which most mass loss has occurred. This observation concludes the multistep reaction mechanism in an air environment. Additionally, there was a link between the pre-exponential values of (A) and activation energy. Higher log A values are more likely to collide and break down during chemical reactions than lower log A values. Compared to the other combinations, RSO + ZDDC + ADDC showed a more noticeable fluctuation in activation energy with conversion. This kind of variance could result from the log chain triglycerides' overlapping thermal

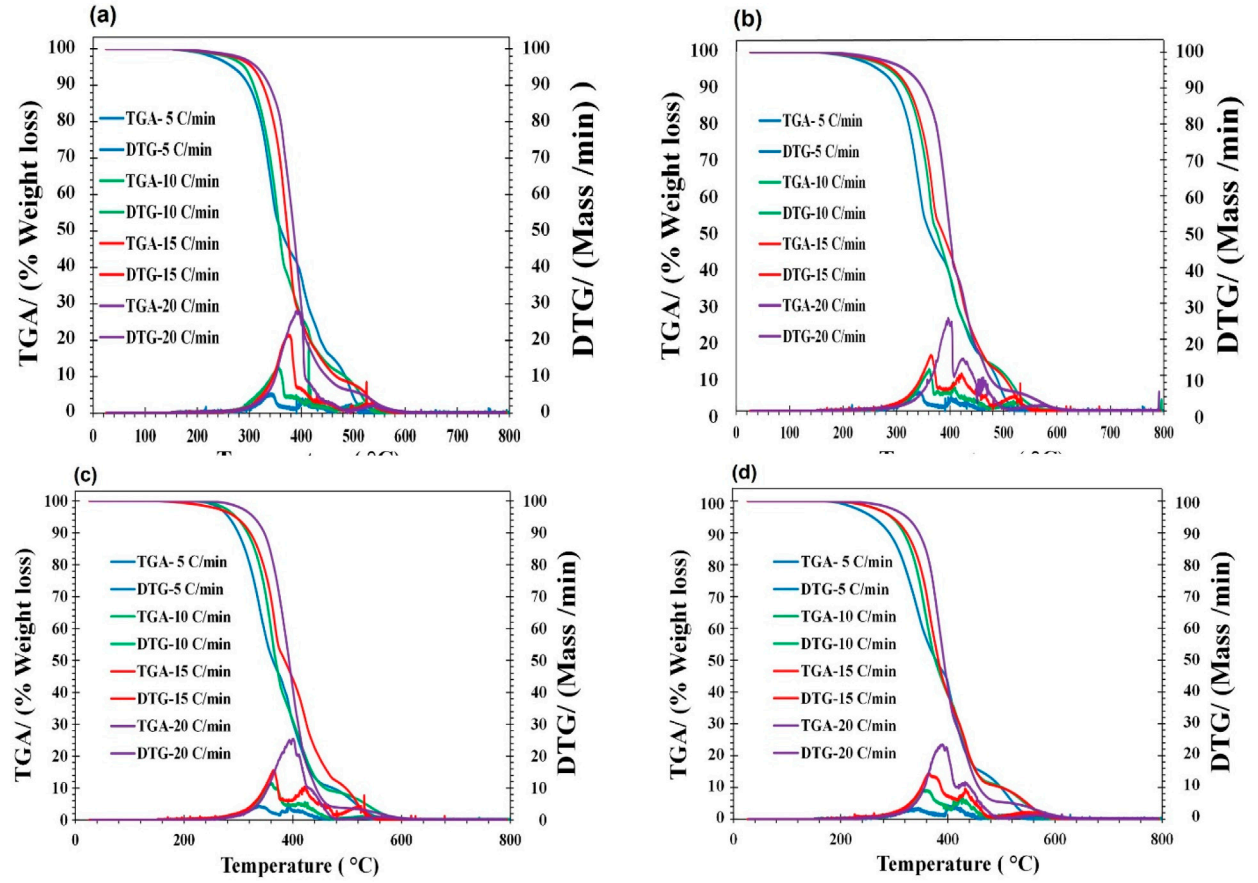

FIGURE 4
TG, DTG curves of synthesized biolubricants: **(A)** HOSO + ZDDC + ADDC **(B)** RSO + ZDDC + ADDC **(C)** HOSO + ZDDP **(D)** RSO + ZDDP.

breakdown response (Sarker et al., 2023). The amount of energy needed by the reactants to complete a particular chemical reaction is known as activation energy (Ea). A higher Ea value indicates that the reaction will be more difficult to carry out. The change in activation energy in each additives indicates that multistep mechanism during an oxidative environment. The higher average activation energy of all additives indicate that these are stable in an oxidative environment. Typically, an ester's oxidative stability is decreased when it has more unsaturation bonds.

3.6 Activation energy and pre-exponential value

The average E_a for each synthesized product was calculated at different conversion fractions while conducting the reaction under air atmospheres. The results are presented in Figure 5 and Table 3. In an air environment, based on the average E_a of each biolubricant product, the thermal stability followed the order: HOSO + ZDDC + ADDC > RSO + ZDDC + ADDC > HOSO + ZDDP > RSO + ZDDP. The highest average E_a was reported at 109.21 kJ/mol (HOSO + ZDDC + ADDC), and the lowest average E_a of RSO + ZDDP (61.50 kJ/mol). The thermal oxidative breakdown of each synthetic product's components which takes place at various temperature ranges, is responsible for the difference in Ea (Sarker et al., 2023).

3.7 Cloud point and pour point

The cloud point, also known as CP, is the temperature at which the oil starts to appear cloudy or begins to precipitate upon cooling. On the other hand, the pour point (PP) is the temperature at which the oil ceases to flow (Kruka et al., 1995), (Gavlin et al.). According to the data presented in Table 2, both RSO and HOSO exhibited similar pour points. However, the addition of ZDDP led to a significant improvement in the pour point for both oils, reducing it from −15°C to −18°C. On the other hand, no notable improvement was observed for RSO, despite the addition of ZDDC and ADDC. For HOSO, the addition of ZDDC and ADDC resulted in the highest improvement in pour point, reducing it from −15°C to −21°C. The variation in the amount of polyunsaturated fatty acids between RSO and HOSO could be a possible reason, with RSO containing higher amount of polyunsaturated fatty acids. (Yosief et al., 2022a), (Yosief et al., 2022b), (Lanjekar and Deshmukh, 2016). The pour points of vegetable oils are lower when they have

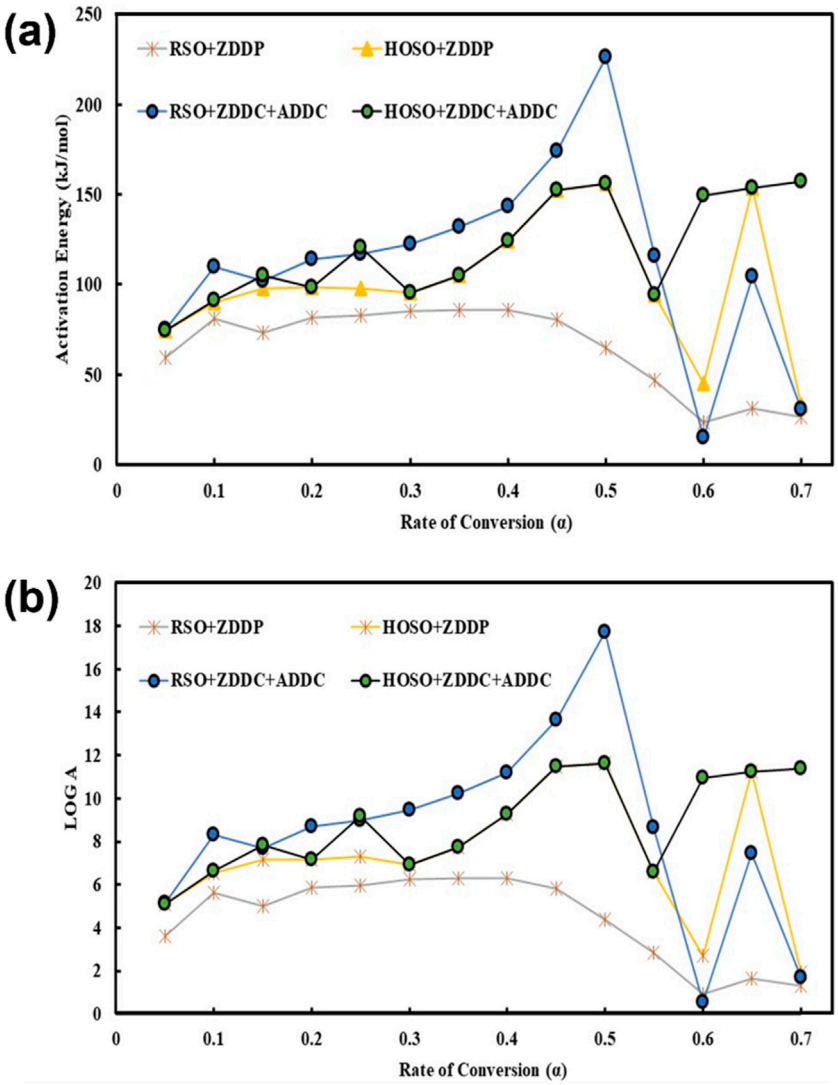

FIGURE 5
Kinetic parameters **(A)** activation energy vs the degree of conversion **(B)** logarithm of preexponential factor vs the degree of conversion.

TABLE 3 Average Activation Energy (E_a) and Pre-exponential factor (A) of base oils and formulated biolubricants under Air.

	E (kj/mol)	log A
RSO	66.72	5.03
HOSO	83.46	6.13
RSO + ZDDP	61.50	4.14
HOSO + ZDDP	98.49	7.12
RSO + ZDDC + ADDC	100.28	7.98
HOSO + ZDDC + ADDC	109.21	8.48

a higher concentration of unsaturated fatty acid chains (Jayadas and Nair, 2006). In regular form, the cloud point of HOSO was lower than that of RSO but a slight improvement in the cloud point could be achieved for both oils by incorporation of additives.

4 Compatibility of additives with base oils

4.1 Coefficient of friction analysis

The coefficients of friction (COF) for RSO, HOSO, and the mixtures of ZDDP with RSO and HOSO are illustrated in Figure 6A. Notably, RSO demonstrated the highest COF, while raw HOSO showed a 9.7% lower COF compared to that of RSO. This difference can likely be attributed to the higher proportion of linoleic acid in RSO. Previous research by Reeves et al. (Yosief et al., 2022b) has observed variations in COF among different biobased oils, which could be explained by differences in their fatty acid compositions. Oils with a lower fraction of oleic acids typically exhibit higher COF values. Upon the addition of the antioxidant additive ZDDP (at a concentration of 1% w/w) to these oils, a noticeable improvement in COF was observed. HOSO with ZDDP demonstrated the lowest COF which was consistent with corresponding micrograph of the

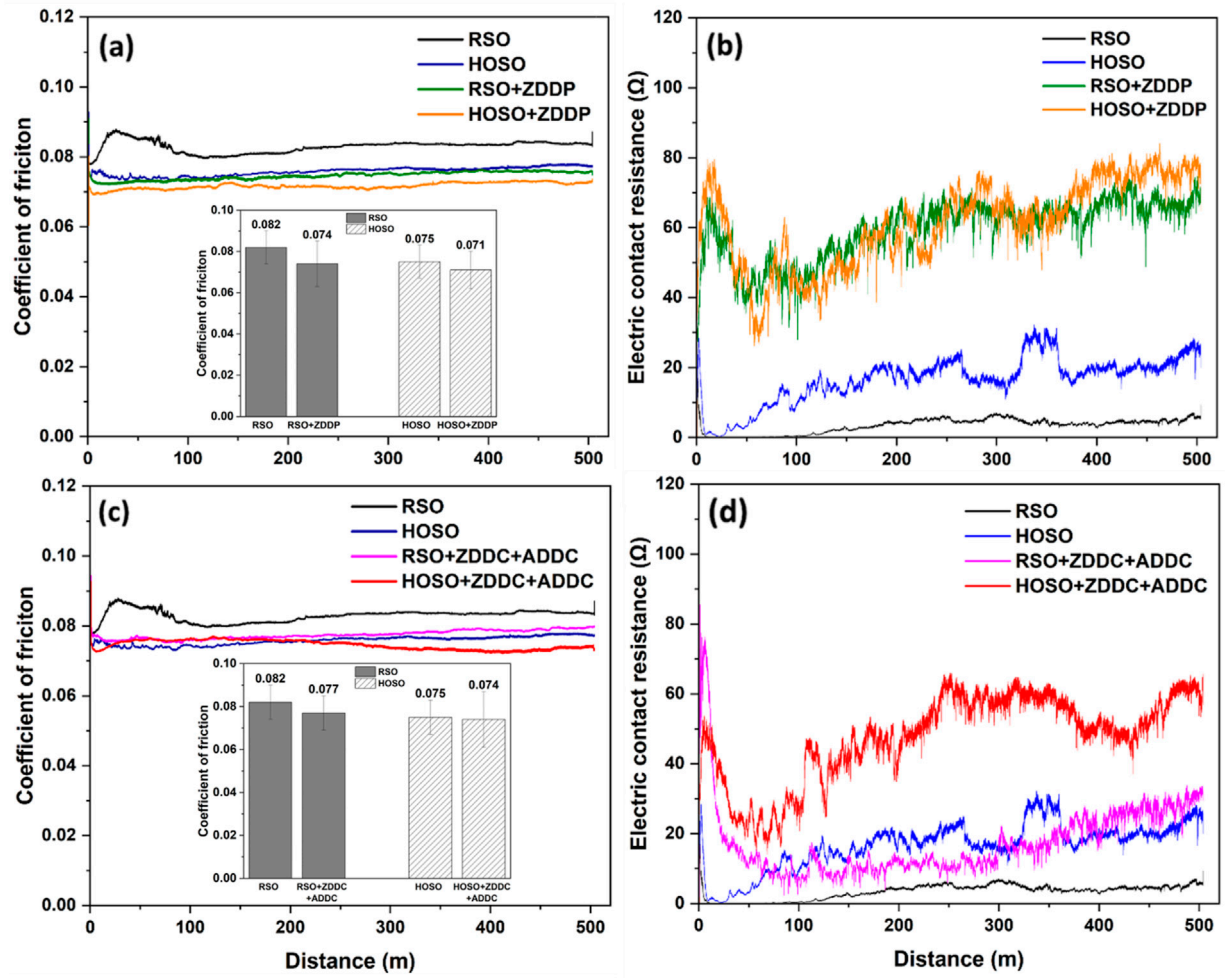

FIGURE 6
Tribological behavior of soybean oils **(A)** coefficient of friction of base oils with ZDDP; **(B)** electric contact resistance of base oils with ZDDP; **(C)** coefficient of friction of base oils with ZDDC and ADDC; **(D)** electric contact resistance of base oils with ZDDC and ADDC.

ball wear (Supplementary Figure S1). The reduction in COF was more pronounced for RSO with ZDDP, amounting to 9.75% against 5.3% for HOSO with ZDDP. When ZDDP was added to RSBO, the CoF decreased at lower sliding speeds, consistent with the findings of Kumar et al. (Kumar et al., 2019).

Electrical Contact Resistance (ECR) measurements offer valuable insights into the formation of an insulating tribofilm within the contact region (Huang et al., 2016). In this study, ECR measurement was conducted to delve deeper into the functional mechanism, acquiring crucial insights into the formation of a protective film at the interface. Figure 6B illustrates the ECR of RSO, HOSO, and ZDDP mixed with RSO and HOSO. Analyzing the results, it became evident that the resistance value for RSO was small, suggesting that it lacked a substantial tribofilm layer. The sliding process induced increased contact between the ball and the flat surface due to the presence of a fragile surface film. This film primarily comprised of iron oxides and underwent a cyclic pattern of formation, breakage, regeneration, and re-rupture, leading to its small resistance value. In contrast, HOSO exhibited a higher resistance value. This elevated resistance value suggested that a tribofilm between the two metal surfaces was obstructing the flow of current, indicating the presence of a thicker or more stable tribofilm compared to the case with RSO. It is noteworthy that tribofilm formation in HOSO appeared to be relatively unstable, which suggests the breakage and formation of tribofilm, but the resistance increased over time. The resistance value for ZDDP mixed with both RSO and HOSO was similar. During the "running-in" period, the resistance value decreased due to interactions between surface asperities. However, after this initial phase, the resistance value increased, indicating the formation of a thicker tribofilm. This thicker tribofilm potentially helped in resulting the lowest coefficient of friction (COF) for the oils with ZDDP. Importantly, the resistance value continued to increase over time, indicating an ongoing tribofilm growth. However, it is worth noting that the tribofilm formation remained moderately stable since not much fluctuation was observed in the trends. Under the application of shear stress, ZDDP can create a thick and protective phosphate glass-based tribofilm on the surface that was in contact, effectively minimizing friction (Zhang and Spikes, 2016).

The Coefficient of Friction (COF) and Electrical contact resistance (ECR) for various oils, including RSO, HOSO and

blends of these oils with antioxidant and antiwear additives (ZDDC and ADDC), are illustrated in Figures 6C, D. When ZDDC was introduced into RSO and HOSO at a concentration of 2% w/w, along with ADDC at the same concentration, an improvement in COF was observed, similar to the results achieved when ZDDP was added. Notably, the COF value for HOSO mixed with ZDDC and ADDC remained similar to raw HOSO. In contrast, RSO experienced a significant 6.1% reduction in friction when combined with ZDDC and ADDC. The thickness of the tribo-film formed by RSO with ZDDC and ADDC was comparable to that of HOSO, as seen in Figure 6D. However, the tribofilm thickness increased over time and reached a stable state for RSO, unlike the case with HOSO. HOSO with ZDDC and ADDC displayed the highest tribo-film thickness but lacked stability. In the ECR signal, some deeper regions or grooves were observed, indicating the breakage of the tribo-film. Such formation and subsequent breakage of the tribofilm, in this case, prevented major reduction in COF. The formation of tribo-films is discussed further in the wear mechanism analysis section.

According to the performance of oils with additives, the additives tended to work better with RSO than with HOSO. This could be attributed to the fact that HOSO contains a lower number of free radicals than RSO, which are produced as a result of the oxidation process. The decomposition of ZDDP in lubricants occurs through three primary mechanisms: thermal (Dickert and Rowe, 1996), (Suominen Fuller et al., 1998), hydrolytic (Watkins, 1982), and oxidative (Mitchell, 1984). Thermal decomposition happens under heat, hydrolytic due to moisture, and oxidative degradation is driven by hydroperoxides and peroxidic radicals. Antioxidants counter these oxidative processes through two key mechanisms. The first one is by radical scavenging, where the antioxidants react with peroxy radicals to prevent the continued propagation of the free radical chain. The second mechanism is through the inhibition of peroxides, where the antioxidants react with hydroperoxide molecules to inhibit the production of peroxy radicals (Zhang and Spikes, 2016), (Spikes), (Azwar Azhari et al., 2015). During these processes, ZDDP molecules and their breakdown products are adsorbed onto metal surfaces, forming a thermal film. Under rubbing conditions, this film transforms into a durable tribofilm, providing wear protection. To ensure strong adhesion and manage iron oxide wear particles, a tribochemical reaction between zinc metaphosphate and iron oxide occurs, leading to the shortening of phosphate chains, a process confirmed by friction tests, which enhances the tribofilm's protective capabilities (Njiwa et al., 2011). In the case of HOSO, the lack of free radicals may hinder the ability of antioxidants to react and create tribofilm, which is a protective layer that reduces wear and friction.

4.2 Wear volume analysis

The comparison of wear volumes observed in flat samples during tribological tests conducted with different additives and base oils is illustrated in Figure 7. Among the oils tested, RSO exhibited the lowest wear resistance. Raw HOSO presented relatively better wear resistance compared to RSO, with an improvement of 8.6%. The difference in wear resistance between HOSO and RSO can be explained by the differences in their respective fatty acid compositions. HOSO contains a higher proportion of oleic acid,

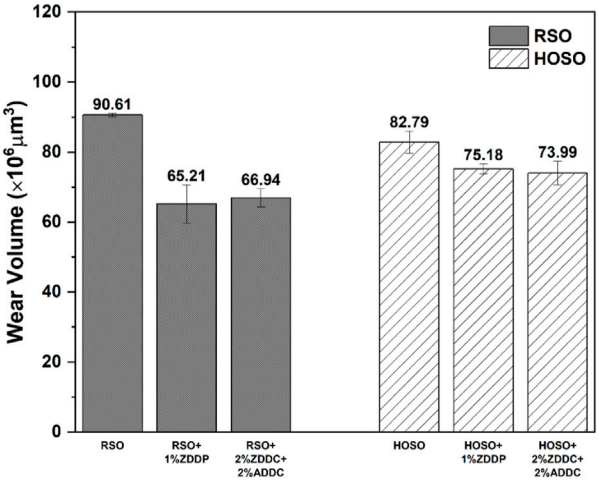

FIGURE 7
Comparative analyses of wear volumes under different lubricated conditions.

a monounsaturated fatty acid with just one double bond in its chain. In contrast, RSO has a lower percentage of oleic acid but a significantly higher percentage of linoleic acid, a polyunsaturated fatty acid with multiple double bonds. Polyunsaturated fatty acids, like linoleic acid, are more susceptible to oxidation due to their multiple double bonds, making them prone to the formation of free radicals and oxidative damage. On the other hand, monounsaturated fatty acids, such as oleic acid, are relatively more stable because they have only one double bond (Siniawski et al., 2007).

The introduction of antioxidant and anti-wear additives to both types of oils resulted in a significant enhancement of wear resistance. Notably, the impact on regular soybean oil (RSO) was more prominent with a remarkable 28% increase in wear resistance, whereas the improvement for HOSO was approximately 9.2%. In the absence of additives, HOSO exhibited better wear resistance, but the introduction of select additives significantly enhanced the wear resistance in RSO compared to HOSO.

The wear depth of the flat samples is depicted in Figure 8,which is a comparison between RSO and RSO with additives, while Figure 8B displays a comparison between HOSO and HOSO with additives. The wear depth was highest in the case of RSO, contributing to the highest wear volume, as discussed earlier in Figure 7. However, Figure 8A shows that wear depth was significantly lower for RSO with additives compared to RSO, which is the primary reason for the lower wear volume discussed earlier. Captured wear depth for HOSO and HOSO with additives was quite similar, which is consistent with the wear volume result.

The wear depth of the balls has been illustrated in Figure 9,which shows the wear depth of RSO and RSO with additives in Figure 9A, while Figure 9B displays the wear depth of HOSO and HOSO with additives. It is worth noting that RSO exhibited the highest wear depth on balls, which confirms the absence of major tribofilm formation. However, there was an improvement in wear resistance of balls when RSO was mixed with additives, although no significant difference was observed between the two additive

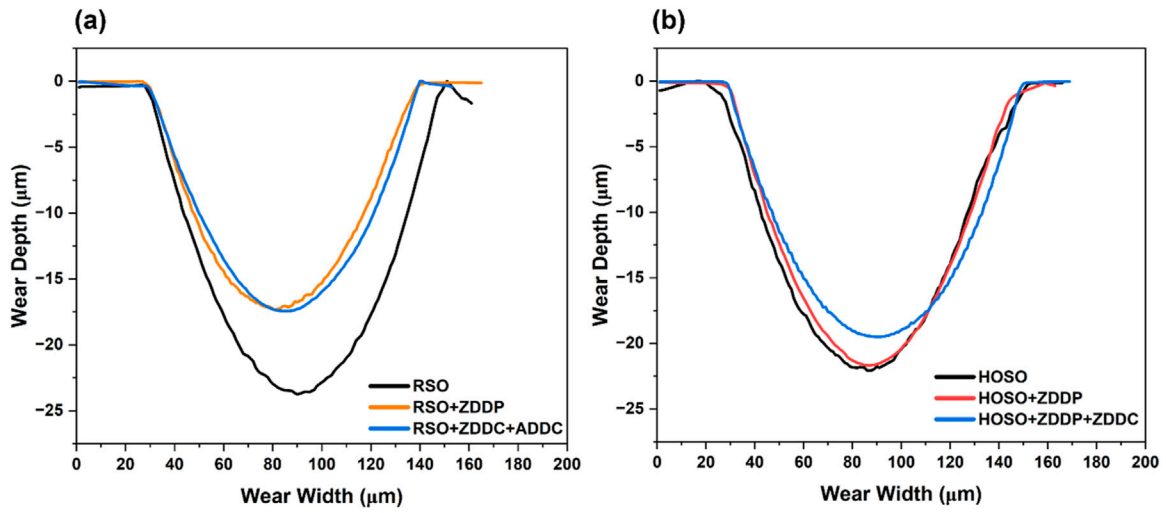

FIGURE 8
2-D Wear depth profile of the wear tracks **(A)** RSO and RSO with additives **(B)** HOSO and HOSO with additives.

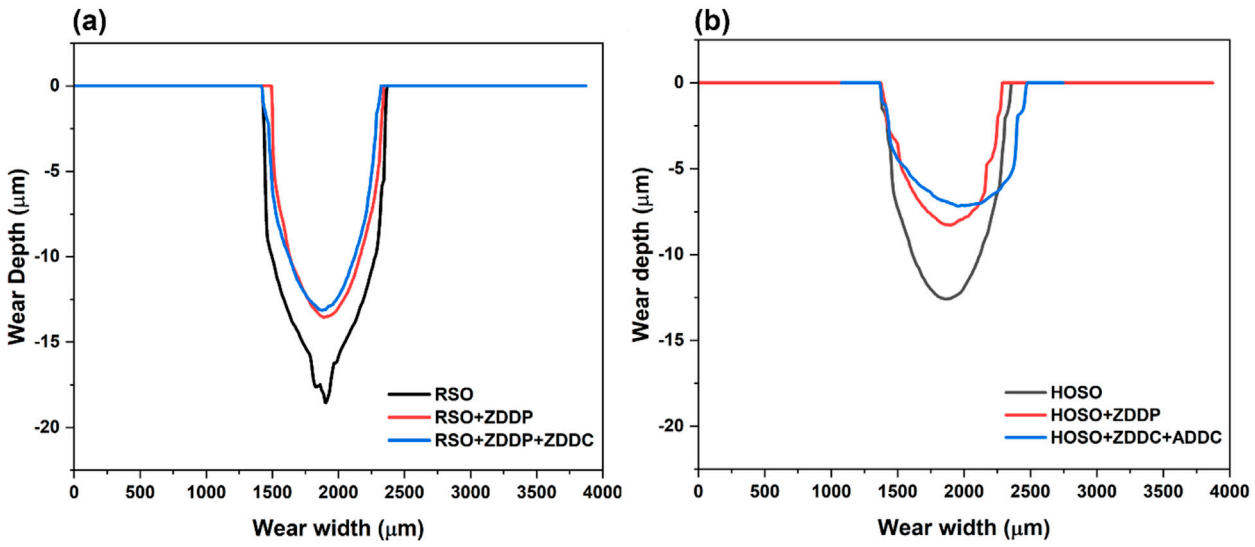

FIGURE 9
2-D Wear depth profile of the balls **(A)** RSO and RSO with additives **(B)** HOSO and HOSO with additives.

cases (ZDDP vs. ZDDC + ADDC). Conversely, HOSO (Figure 9B) showed less wear depth compared to RSO. Moreover, HOSO with additives exhibited the lowest wear depth.

4.3 Wear mechanism analysis

The SEM images and EDS elemental mapping micrographs captured from work out regions of AISI 52100 flat samples are presented in Figure 10. The micrographs from the ball wear were not captured due to difficulty in recording reasonable micrographs considering significantly low order of wear volume as compared to flat samples. The predominant wear mechanism observed in the flat tracks was abrasive wear. Abrasive wear refers to the removal of small particles from one or both surfaces due to the presence of harder abrasive particles or materials (Saha and Roy, 2023), (Hyunsuk Choi Piash Bhowmik and Roy, 2024). However, there was no significant evidence of material transfer from the balls to the flats, as both were made of the same material. The wear tracks using RSO and HOSO without additives did not show any cracks, dislodged or spalling of materials, as visible in Figures 10A, D. The EDS mapping revealed that both oils formed an oxide layer (tribo-layer), but it was higher for HOSO compared to RSO. HOSO had a greater electric contact resistance compared to RSO, as observed in Figures 6B, D. This can be attributed to the higher amount of oxide layer formation in HOSO compared to RSO. RSO

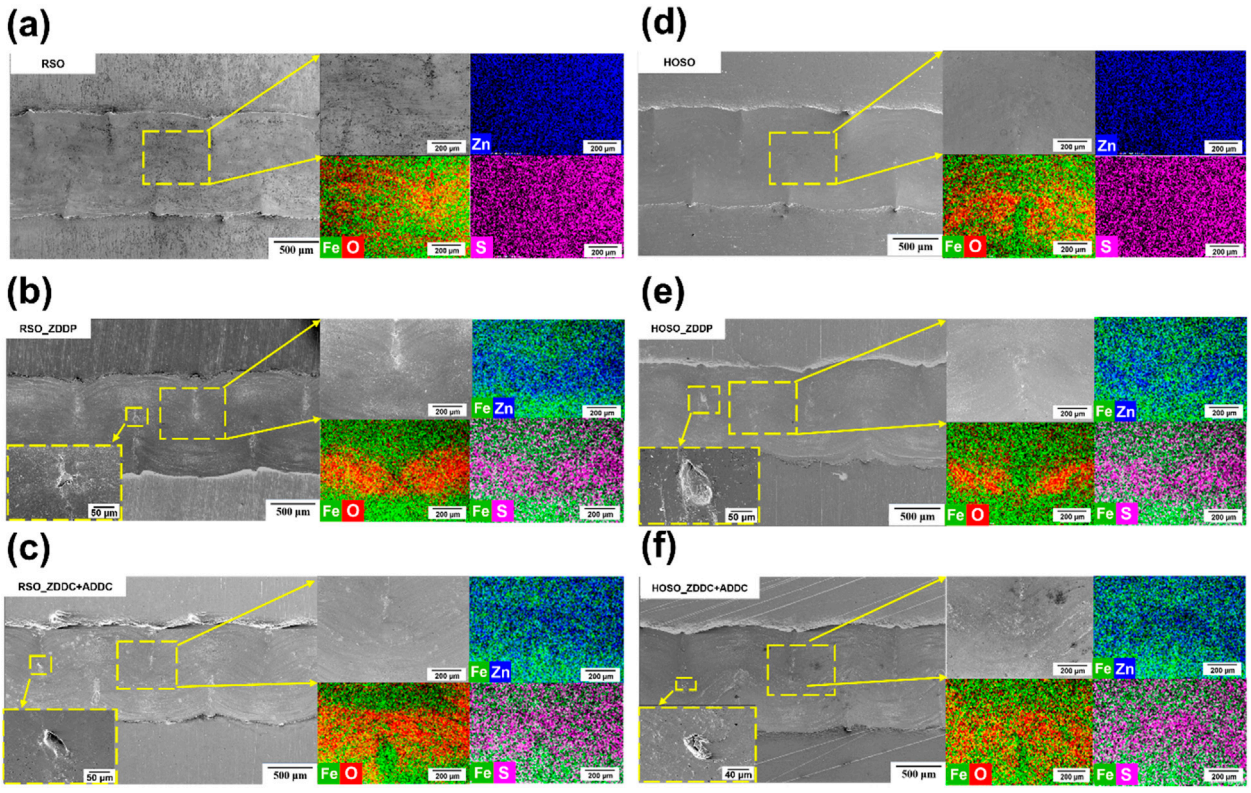

FIGURE 10
SEM & EDS images of wear tracks on the flat samples **(A)** RSO, **(B)** RSO with ZDDP, **(C)** RSO with ZDDC and ADDC, **(D)** HOSO, **(E)** HOSO with ZDDP and **(F)** HOSO with ZDDC and ADDC at room temperature. Representative images show the wear tracks' morphology and wear mechanism after the sliding tests.

with ZDDP, ZDDC, and ADDC additives showed similar characteristics, with the visible formation of a thick tribo-layer of oxygen (O), zinc (Zn), and sulfur(S), as seen in Figures 10B,C. The formation of Zn and S tribo-oxide layers can be attributed to the presence of these elements in ZDDP and ZDDC. ZDDP additives are known to create a protective tribofilm layer on metal surfaces during lubrication. ZDDP reacts with metal surfaces to create phosphorus-containing compounds that aid in the formation of the tribofilm. The tribofilm can consist of a mixture of compounds, including zinc phosphate, iron phosphate, and other reaction products (Zhang and Spikes, 2016), (Spikes). Sharma et al. (Sharma et al., 2007) studied the synergistic effect of ZDDC and ADDC, demonstrating that the combination of ZDDC and ADDC has been shown to significantly enhance the antioxidant performance of soybean oil, with the oxidation induction time increasing from 12 min to 45 min when both additives are used together. The hypothesis is that the hydroperoxide decomposition may lead to the formation of different sulfur oxyacids due to the presence of sulfur in metal dithiocarbamates. These acids can potentially play a role in the antioxidant mechanism by decomposing hydroperoxides. Another possible explanation is a recycling mechanism that allows for partial recovery of ZDDC or ADDC from their oxidized versions by scavenging peroxy radicals or decomposing hydroperoxides. It is likely that a reaction sequence involving metal dialkyldithiocarbamate via oxidized dialkyldithiocarbamates and a further oxidized metal complex with antioxidant ability, possibly aided by sulfur dioxide, accounts for the observed synergistic antioxidant activity (Holcik et al., 1983), (Sexton), (Howard and Tong'), (Burn et al.). The presence of ADDC further stabilizes the antioxidant system by forming stable intermediate radicals during its reaction with ZDDC, enhancing overall stability and efficiency. The electrical contact resistance also showed a higher resistance due to the formation of this thick tribo-layer, further validating the effectiveness of these additives in providing superior wear protection. Minor dislodged or spelling of material was observed in both cases. Similarly, HOSO with additives (Figures 10E, F) also exhibited minor spalling of materials in the wear tracks, along with the formation of a thick tribo-layer. However, the tribo-layer was thicker in RSO with additives than in HOSO with additives, as visible in the elemental mapping images and electric contract resistance plots discussed earlier in Figure 6. In the absence of additives, the wear tracks exhibited a smooth surface. This phenomenon can be attributed to micro-cutting, a process in which the material is cut at a microscopic level, leading to a smoothing effect on the surface (Kočović et al.). On the other hand, when additives were used, a thicker tribofilm was formed, which resulted in ploughing within the wear track. This ploughing might be the likely cause of the observed spalling or dislodging of material.

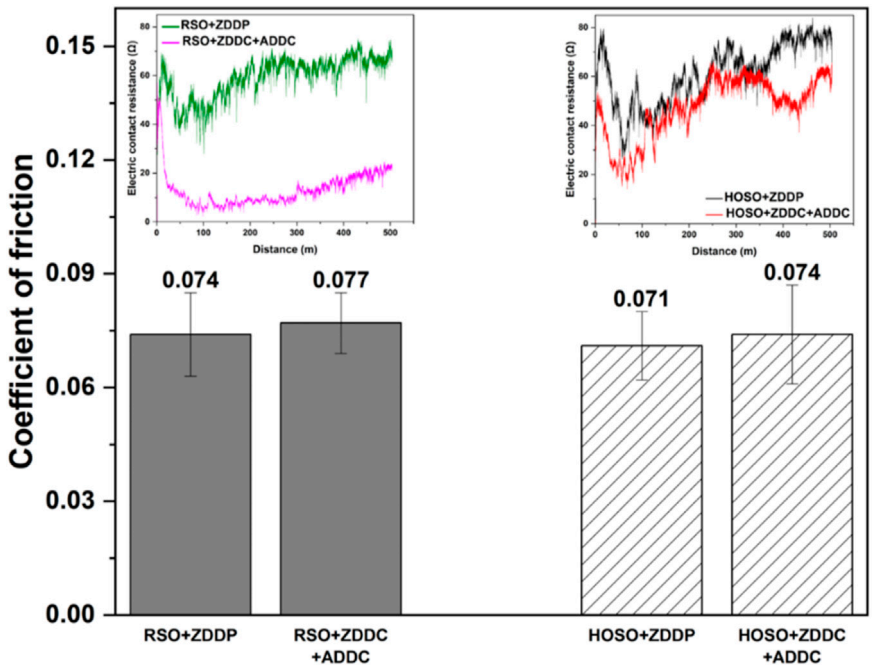

FIGURE 11
Comparison of coefficient of friction of base oils with additives.

4.4 Revealing the best performing additive to soybean oils

The results of the wear analysis indicate that the performance of ZDDP and the combination of ZDDC with ADDC is similar when used with both RSO and HOSO as lubricants. In terms of the coefficient of friction, ZDDP exhibited a slightly better performance compared to the combination of ZDDC and ADDC. The visual representation of the coefficient of friction for RSO and HOSO when paired with ZDDP and the ZDDC and ADDC mixture is depicted in Figure 11. It is evident that RSO and HOSO when combined with ZDDP, exhibited approximately 4% lower coefficient of friction (COF) compared to when paired with the ZDDC and ADDC mixture. This indicates that ZDDP is advantageous in reducing friction when used with both RSO and HOSO as lubricants in the tribological tests. Inserted images show that ZDDP created a thicker and more stable tribofilm than the mixture of ZDDC and ADDC since the contact resistance value was higher for ZDDP and the trends were stable. RSO with ZDDC and ADDC had lower electrical contact resistance, indicating a thinner tribofilm. On the other hand, HOSO with ZDDC and ADDC appeared to have a potentially thicker tribofilm. Still, the presence of instability and grooves suggests a continuous process of tribofilm formation and breakage, which might be the reason for the higher COF value.

5 Conclusion

The tribological and physicochemical properties of regular soybean oil (RSO) and high oleic soybean oil (HOSO), mixed with two distinct types of antioxidants and anti-wear additives, namely, ZDDP and a combination of ZDDC and ADDC, were analyzed. The major findings are listed below.

- Lubricants formulated with HOSO showed higher oxidative stability than those formulated with RSO due to the lower unsaturation levels in HOSO. The combination of ZDDC + ADDC additives provided higher oxidative stability than the ZDDP additive. The lubricant formulated with HOSO and the ZDDC + ADDC additive combination demonstrated the highest oxidative stability. This could be due to the presence of both ZDDC (antioxidant) and ADDC (antiwear) additives, whereas ZDDP is primarily used as an antiwear additive.
- RSO showed the highest COF, while HOSO had a 9.7% lower COF than RSO, potentially due to the higher proportion of linoleic acid in RSO. The addition of the antioxidant additive ZDDP led to a noticeable improvement in COF for both RSO and HOSO. ECR measurements showed that RSO had a small resistance value, indicating a lack of substantial tribofilm layer, while HOSO exhibited a higher resistance value, suggesting the presence of a thicker tribofilm compared to RSO. The resistance value for both RSO and HOSO when ZDDP was added was similar, indicating the formation of a thicker tribofilm, which resulted in the lowest COF for the oils with ZDDP. Additives worked better with RSO than HOSO, likely due to the lower amount of free radicals formed during HOSO use, hindering the ability of antioxidants to react and create tribofilm.
- HOSO presented better wear resistance compared to RSO due to its higher percentage of oleic acid, a more stable monounsaturated fatty acid. However, the introduction of

antioxidant and anti-wear additives significantly enhances wear resistance in both oils, with RSO experiencing a more significant improvement of 28% compared to HOSO's 9.2%. The wear depth analysis of flat samples shows that wear depth is highest in RSO but significantly lower when used with additives. In contrast, HOSO and HOSO with additives show similar wear depth, consistent with the wear volume result. The wear depth of the balls was highest for RSO, indicating the absence of tribofilm formation. However, the wear depth in RSO improved when used with additives, but no significant difference was observed between the additives. In contrast, HOSO exhibited less wear depth compared to RSO, and HOSO with additives showed the lowest wear depth.

- Abrasive wear was the predominant wear mechanism observed in flat tracks. Both RSO and HOSO oils formed an oxide layer (tribofilm), but it was higher for HOSO compared to RSO. RSO and HOSO with additives showed the visible formation of a thick tribo-layer of oxygen, zinc, and sulfur, providing superior wear protection. The performance of ZDDP and the combination of ZDDC with ADDC is similar when used with RSO and HOSO as lubricants. However, ZDDP slightly outperformed the mixture in terms of COF, which was reduced by approximately 4% when RSO and HOSO were combined with ZDDP compared to the ZDDC and ADDC mixture, indicating that ZDDP was advantageous in reducing friction in tribological tests.

Biobased lubricants, like those from soybean oil, are eco-friendly and ideal for industries like agriculture, automotive, marine, construction, and renewable energy. They reduce environmental risks, offering sustainable alternatives for engines, hydraulic systems, and heavy equipment. Raw HOSO provides better friction and wear behavior compared to RSO, but our conducted research indicates that the addition of antioxidant and anti-wear additives leads to a much greater improvement in friction and wear performance when these are mixed with RSO as compared that of HOSO. Overall, this investigation will play a crucial role for future scientists and engineers formulating soybean based lubricating oil for target applications. This presents some guidelines on selection of key lubricant additives and their compatibility with both regular and high oleic soybean oil version. Depending on their primary goal (wear resistance or friction resistance) and availability of base feedstock, they can tune the major lubricant additives in the fully formulated versions.

Data availability statement

The raw data supporting the conclusions of this article will be made available by the authors, without undue reservation.

Author contributions

PB: Formal Analysis, Investigation, Methodology, Writing–original draft. BS: Formal Analysis, Methodology, Supervision, Writing–review and editing. MS: Formal Analysis, Investigation, Methodology, Writing–review and editing. KM: Investigation, Methodology, Writing–review and editing. YW: Resources, Supervision, Writing–review and editing. CT: Methodology, Resources, Writing–review and editing. SR: Conceptualization, Funding acquisition, Project administration, Resources, Supervision, Writing–review and editing.

Funding

The author(s) declare that financial support was received for the research, authorship, and/or publication of this article. The authors express their gratitude to the North Dakota Soybean Council for generously providing the funding that supported the research endeavors.

Acknowledgments

The authors would like to extend their sincere gratitude to Jay Evenstad from the University of North Dakota for his invaluable support in fabricating the sample holder for the tribological testing. His contribution has been crucial in making this research a success. The authors express their gratitude to the North Dakota Soybean Council for generously providing the funding that supported the research endeavors.

Conflict of interest

The authors declare that the research was conducted in the absence of any commercial or financial relationships that could be construed as a potential conflict of interest.

Publisher's note

Author disclaimer

Mention of trade names or commercial products in this article is solely for the purpose of providing specific information and does not imply recommendation or endorsement by the U.S. Department of Agriculture (USDA). USDA is an equal opportunity provider and employer.

Supplementary material

The Supplementary Material for this article can be found online at: https://www.frontiersin.org/articles/10.3389/fmech.2024.1488407/full#supplementary-material

References

Adhvaryu, A., and Erhan, S. Z. (2002). Epoxidized soybean oil as a potential source of high-temperature lubricants. *Ind. Crops Prod.* 15, 247–254. doi:10.1016/s0926-6690(01)00120-0

Adhvaryu, A., Erhan, S. Z., and Perez, J. M. (2004). Tribological studies of thermally and chemically modified vegetable oils for use as environmentally friendly lubricants. *Wear* 257 (3–4), 359–367. doi:10.1016/j.wear.2004.01.005

Adhvaryu, A., Liu, Z., and Erhan, S. Z. (2005). Synthesis of novel alkoxylated triacylglycerols and their lubricant base oil properties. *Ind. Crops Prod.* 21 (1), 113–119. doi:10.1016/j.indcrop.2004.02.001

Azwar Azhari, M., Fathe'li, M. A., Aziz, N., Nadzri, M. M., and Yusuf, Y. (2015). A review on addition of Zinc Dialkyldithiophosphate in vegetable oil as physical properties improver. 10. Available at: www.arpnjournals.com.

Bahari, A., Lewis, R., and Slatter, T. (2018). Friction and wear phenomena of vegetable oil–based lubricants with additives at severe sliding wear conditions. *Tribol. Trans.* 61 (2), 207–219. doi:10.1080/10402004.2017.1290858

Bhadeshia, H. K. D. H. (2012). Steels for bearings. *Prog. Mater. Sci.* 57, 268–435. doi:10.1016/j.pmatsci.2011.06.002

Bhowmik, P., Sharma, B. K., Sarker, M. I., Choi, H., Tang, C., and Roy, S. (2024). Investigating the impact of a newly developed chemical modification technique on improving the tribological properties of high oleic soybean oil. *Sustain Energy Fuels* 8, 1314–1328. doi:10.1039/D3SE01526B

Burn, A. J., Dewan, S. K., Gosney, I., and Tan, P. S. G. (2011) "Phosphorus-31 nuclear magnetic resonance study of the mechanism and kinetics of the hydrolysis of zinc(ii) 0,O-diethyl dithiophosphate and some related com po u nds."

Cermak, S. C., Isbell, T. A., Bredsguard, J. W., and Thompson, T. D. (2017). "Chapter 14 - estolides: Synthesis and Applications**Mention of trade names or commercial products in this publication is solely for the purpose of providing specific information and does not imply recommendation or endorsement by the U.S. Department of Agriculture. USDA is an equal opportunity provider and employer," in *Fatty acids*. Editor M. U. Ahmad (AOCS Press), 431–475. doi:10.1016/B978-0-12-809521-8.00015-5

Cheenkachorn, K. (2013). "A study of wear properties of different soybean oils," in *Energy procedia* (Elsevier Ltd), 633–639. doi:10.1016/j.egypro.2013.11.065

Dickert, J. J., and Rowe, C. N. (1996). Thermal decomposition of metal O,O-dialkyl phosphorodithioates. *J. Org. Chem.* 32, 647–653. doi:10.1021/jo01278a031

Fang, H. L., and Mccormick, R. L. 2006, "Spectroscopic study of biodiesel degradation pathways," , doi:10.4271/2006-01-3300

Fox, N. J., and Stachowiak, G. W. (2007). Vegetable oil-based lubricants-A review of oxidation. *Tribol. Int.* 40 (7), 1035–1046. doi:10.1016/j.triboint.2006.10.001

Fox, N. J., Tyrer, B., and Stachowiak, G. W. (2004). Boundary lubrication performance of free fatty acids in sunflower oil. *Tribol. Lett.* 16, 275–281. doi:10.1023/b:tril.0000015203.08570.82

Gavlin, G., Swire, E. A., and Jones, S. P., (2021) "Pour point depression of lubricating oils 6 0."

Giakoumis, E. G., and Sarakatsanis, C. K. (2018). Estimation of biodiesel cetane number, density, kinematic viscosity and heating values from its fatty acid weight composition. *Fuel* 222, 574–585. doi:10.1016/j.fuel.2018.02.187

Hamnas, A., and Unnikrishnan, G. (2023). *Bio-lubricants from vegetable oils: characterization, modifications, applications and challenges – review*. Elsevier Ltd. doi:10.1016/j.rser.2023.113413

Holcik, J., Koenig, J. L., and Shelton, J. R., "The antioxidant activity of phosphorus compounds Part I: decomposition of hydroperoxides by pentaerythritol diphosphites," 1983.

Hong, I. K., Jeon, G. S., and Lee, S. B. (2014). Prediction of biodiesel fuel properties from fatty acid alkyl ester. *J. Industrial Eng. Chem.* 20 (4), 2348–2353. doi:10.1016/j.jiec.2013.10.011

Howard, J. A., and Tong, N. D. S.-B. (2022) Metal complexes as antioxidants. ' 7. Kinetics of inhibition of styrene autsxidakiola by zinc di-isopropyldithiophosphate. Available at: www.nrcresearchpress.com.

Huang, G., Yu, Q., Cai, M., Zhou, F., and Liu, W. (2016). Highlighting the effect of interfacial interaction on tribological properties of supramolecular gel lubricants. *Adv. Mater Interfaces* 3 (3). doi:10.1002/admi.201500489

Hwang, H. S., and Erhan, S. Z. (2006). Synthetic lubricant basestocks from epoxidized soybean oil and Guerbet alcohols. *Ind. Crops Prod.* 23 (3), 311–317. doi:10.1016/j.indcrop.2005.09.002

Hyunsuk Choi Piash Bhowmik, T. R. Y. B. Y. W., and Roy, S. (2024). Exploring the friction and wear mechanisms of nickel titanium alloy fabricated by laser powder and wire-based directed energy deposition. *Tribol. Trans.* 0 (0), 1–16. doi:10.1080/10402004.2024.2358507

Jayadas, N. H., and Nair, K. P. (2006). Coconut oil as base oil for industrial lubricants-evaluation and modification of thermal, oxidative and low temperature properties. *Tribol. Int.* 39 (9), 873–878. doi:10.1016/j.triboint.2005.06.006

Jayadas, N. H., Prabhakaran Nair, K., and G, A. (2007). Tribological evaluation of coconut oil as an environment-friendly lubricant. *Tribol. Int* 40 (2), 350–354. doi:10.1016/j.triboint.2005.09.021

Kočović, V., Džunić, D., Savić, S. P., Bijelić, I., Miljanić, D., and Vukelić, D. "Serbian tribology society serbiatrib '23 18 th international conference on tribology optimization of the MICRO-CUTTING process in order to reduce the surface roughness."

Kruka, V. R., Cadena, E. R., and Long, T. E. (1995). Cloud-point determination for crude oils. *J. Petroleum Technol.* 47, 681–687. doi:10.2118/31032-pa

Kumar, R., and Gautam, R. K. (2022). Tribological investigation of sunflower and soybean oil with metal oxide nanoadditives. *Biomass Convers. Biorefin* 14, 2389–2401. doi:10.1007/s13399-022-02411-6

Kumar Chaurasia, S., Kumar Singh, N., and Kumar Singh, L. (2020). Friction and wear behavior of chemically modified Sal (Shorea Robusta) oil for bio based lubricant application with effect of CuO nanoparticles. *Fuel* 282, 118762. doi:10.1016/j.fuel.2020.118762

Kumar, G., Garg, H. C., and Gijawara, A. (2019). Experimental investigation of tribological effect on vegetable oil with CuO nanoparticles and ZDDP additives. *Industrial Lubr. Tribol.* 71 (3), 499–508. doi:10.1108/ILT-05-2018-0196

Kumar, N. (2017), Oxidative stability of biodiesel: causes, effects and prevention, 15. *Elsevier Ltd*. doi:10.1016/j.fuel.2016.11.001

Lanjekar, R. D., and Deshmukh, D. (2016). *A review of the effect of the composition of biodiesel on NOx emission, oxidative stability and cold flow properties*. Elsevier Ltd. doi:10.1016/j.rser.2015.10.034

Masjuki, H. H., Maleque, M. A., Kubo, A., and Nonaka, T. (1999). Palm oil and mineral oil based lubricants-their tribological and emission performance. Available at: www.elsevier.com/locate/triboint.

McNutt, J., and He, Q. S. (2016). Development of biolubricants from vegetable oils via chemical modification. *Korean Soc. Industrial Eng. Chem.* 36, 1–12. doi:10.1016/j.jiec.2016.02.008

Milano, J., Shamsuddin, A. H., Silitonga, A., Sebayang, A., Siregar, M. A., Masjuki, H., et al. (2022). Tribological study on the biodiesel produced from waste cooking oil, waste cooking oil blend with *Calophyllum inophyllum* and its diesel blends on lubricant oil. *Energy Rep.* 8, 1578–1590. doi:10.1016/j.egyr.2021.12.059

Mitchell, P. C. H. (1984). Oil-soluble MO-S compounds as lubricant additives. *Wear* 100 (1), 281–300. doi:10.1016/0043-1648(84)90017-6

Mousavi, S. B., and Zeinali Heris, S. (2020). Experimental investigation of ZnO nanoparticles effects on thermophysical and tribological properties of diesel oil. *Int. J. Hydrogen Energy* 45 (43), 23603–23614. doi:10.1016/j.ijhydene.2020.05.259

Mousavi, S. B., Zeinali Heris, S., and Hosseini, M. G. (2019). Experimental investigation of MoS2/diesel oil nanofluid thermophysical and rheological properties. *Int. Commun. Heat Mass Transf.* 108 (Nov), 104298. doi:10.1016/j.icheatmasstransfer.2019.104298

Mousavi, S. B., Heris, S. Z., and Estellé, P. (2020). Experimental comparison between ZnO and MoS2 nanoparticles as additives on performance of diesel oil-based nano lubricant. *Sci. Rep.* 10 (1), 5813. doi:10.1038/s41598-020-62830-1

Mousavi, S. B., Zeinali Heris, S., and Estellé, P. (2021). Viscosity, tribological and physicochemical features of ZnO and MoS2 diesel oil-based nanofluids: an experimental study. *Fuel* 293 (Jun), 120481. doi:10.1016/j.fuel.2021.120481

Mousavi, S. B., Pourpasha, H., and Heris, S. Z. (2024). High-temperature lubricity and physicochemical behaviors of synthesized Cu/TiO2/MnO2-doped GO nanocomposite in high-viscosity index synthetic biodegradable PAO oil. *Int. Commun. Heat Mass Transf.* 156 (Aug), 107642. doi:10.1016/j.icheatmasstransfer.2024.107642

Napolitano, G. E., Ye, Y., and Cruz-Hernandez, C. (2018). Chemical characterization of a high-oleic soybean oil. *JAOCS, J. Am. Oil Chemists' Soc.* 95 (5), 583–589. doi:10.1002/aocs.12049

Njiwa, P., Minfray, C., Le Mogne, T., Vacher, B., Martin, J. M., Matsui, S., et al. (2011). Zinc dialkyl phosphate (ZP) as an anti-wear additive: comparison with ZDDP. *Tribol. Lett.* 44 (1), 19–30. doi:10.1007/s11249-011-9822-6

Okafor, A. C., and Nwoguh, T. O. (2020). A study of viscosity and thermal conductivity of vegetable oils as base cutting fluids for minimum quantity lubrication machining of difficult-to-cut metals. *Int. J. Adv. Manuf. Technol.* 106 (3–4), 1121–1131. doi:10.1007/s00170-019-04611-3

Ouyang, T., Lei, W., Tang, W., Shen, Y., and Mo, C. (2021). Experimental investigation of the effect of IF-WS2 as an additive in castor oil on tribological property. *Wear* 486-487, 204070–204487. doi:10.1016/j.wear.2021.204070

Qin, W., Wang, M., Sun, W., Shipway, P., and Li, X. (2019). Modeling the effectiveness of oil lubrication in reducing both friction and wear in a fretting contact. *Wear* 426–427, 770–777. doi:10.1016/j.wear.2019.02.029

Ramírez-Verduzco, L. F., Rodríguez-Rodríguez, J. E., and Jaramillo-Jacob, A. D. R. (2012). Predicting cetane number, kinematic viscosity, density and higher heating value of biodiesel from its fatty acid methyl ester composition. *Fuel* 91 (1), 102–111. doi:10.1016/j.fuel.2011.06.070

Ravasio, N., Zaccheria, F., Gargano, M., Recchia, S., Fusi, A., Poli, N., et al. 2002. Environmental friendly lubricants through selective hydrogenation of rapeseed oil over supported copper catalysts, 233, 1, 6. doi:10.1016/s0926-860x(02)00128-x

Reeves, C. J., and Menezes, P. L. (2017). Evaluation of boron nitride particles on the tribological performance of avocado and canola oil for energy conservation and sustainability. *Int. J. Adv. Manuf. Technol.* 89 (9–12), 3475–3486. doi:10.1007/s00170-016-9354-1

Reeves, C. J., Siddaiah, A., and Menezes, P. L. (2017). *Ionic liquids: a plausible future of bio-lubricants*. Springer International Publishing. doi:10.1007/s40735-017-0076-1

Roy, S., Jazaa, Y., and Sundararajan, S. (2019). Investigating the micropitting and wear performance of copper oxide and tungsten carbide nanofluids under boundary lubrication. *Wear* 428–429, 55–63. doi:10.1016/j.wear.2019.03.007

Roy, S., Speed, L., Viola, M., Luo, H., Leonard, D., and Qu, J. (2021). Oil miscible phosphonium-phosphate ionic liquid as novel antiwear and antipitting additive for low-viscosity rear axle lubricants. *Wear* 466–467, 203588. doi:10.1016/j.wear.2020.203588

Ruggiero, A., D'Amato, R., Merola, M., Valašek, P., and Müller, M. (2017). Tribological characterization of vegetal lubricants: comparative experimental investigation on Jatropha curcas L. oil, Rapeseed Methyl Ester oil, Hydrotreated Rapeseed oil. *Tribol. Int.* 109, 529–540. doi:10.1016/j.triboint.2017.01.030

Saha, S., and Roy, S. (2023). *Metallic dental implants wear mechanisms, materials, and manufacturing processes: a literature review*. MDPI. doi:10.3390/ma16010161

Sahasrabudhe, S. N., Rodriguez-Martinez, V., O'Meara, M., and Farkas, B. E. (2017). Density, viscosity, and surface tension of five vegetable oils at elevated temperatures: measurement and modeling. *Int. J. Food Prop.* 20, 1–17. doi:10.1080/10942912.2017.1360905

Sarker, M. I., Mainali, K., Sharma, B. K., Yadav, M. P., Ngo, H., and Ashby, R. D. (2023). Synthesized biolubricants from naturally derived oleic acid: oxidative stability and cold flow performance. *Ind. Crops Prod.* 204 (Nov), 117315. doi:10.1016/j.indcrop.2023.117315

Seppanen, C. M., Song, Q., and Saari Csallany, A. (2010) "The antioxidant functions of tocopherol and tocotrienol homologues in oils," in *fats, and food systems*. doi:10.1007/s11746-009-1526-9

Sexton, M. (2011) "Mechanisms of antioxidant action. Part 4,' the decomposition of 1-methyl4-phenylethyl hydroperoxide by zinc dialkyldithiocarbamates and zinc xanthates."

Sharma, B. K., Perez, J. M., and Erhan, S. Z. (2007). Soybean oil-based lubricants: a search for synergistic antioxidants. *Energy Fuels* 21 (4), 2408–2414. doi:10.1021/ef0605854

Sharma, B. K., Rashid, U., Anwar, F., and Erhan, S. Z. (2009). Lubricant properties of Moringa oil using thermal and tribological techniques. *J. Therm. Anal. Calorim.* 96 (3), 999–1008. doi:10.1007/s10973-009-0066-8

Shodji Tamada, I., Renato, P., Lopes, M., Montagnolli, R. N., and Bidoia, E. D. (2012). Biodegradation and toxicological evaluation of lubricant oils. *Arch. Biol. Technol. V.* 55 (6), 951–956. doi:10.1590/s1516-89132012000600020

Shomchoam, B., and Yoosuk, B. (2014). Eco-friendly lubricant by partial hydrogenation of palm oil over Pd/γ-Al2O3 catalyst. *Ind. Crops Prod.* 62, 395–399. doi:10.1016/j.indcrop.2014.09.022

Siniawski, M. T., Saniei, N., Adhikari, B., and Doezema, L. A. (2007). Influence of fatty acid composition on the tribological performance of two vegetable-based lubricants. *J. Synthetic Lubr.* 24 (2), 101–110. doi:10.1002/jsl.32

Spikes, H. (2007). The history and mechanisms of ZDDP."

Standard Practice for calculating viscosity (2024). Standard Practice for calculating viscosity index from kinematic viscosity at 40°C and 100°C 1. doi:10.1520/D2270-10R16

Standard test method for cloud point of petroleum (2023). Standard test method for cloud point of petroleum products and liquid fuels (constant cooling rate method) 1. doi:10.1520/D5773-21

Standard test method for density, relative density (2022). Standard test method for density, relative density, and API gravity of liquids by digital density meter 1. doi:10.1520/D4052-18A

Standard test method for dynamic viscosity (2021). Standard test method for dynamic viscosity and density of liquids by stabinger viscometer (and the calculation of kinematic viscosity) 1. doi:10.1520/D7042-21

Standard test method for pour point of petroleum (2020). Standard test method for pour point of petroleum products (automatic pressure pulsing method) 1. doi:10.1520/D5949-16R22

Suominen Fuller, M. L., Kasrai, M., Bancroft, G. M., Fyfe, K., and Tan, K. H. (1998). Solution decomposition of zinc dialkyl dithiophosphate and its effect on antiwear and thermal film formation studied by X-ray absorption spectroscopy. *Tribol. Int.* 31, 627–644. doi:10.1016/s0301-679x(98)00084-x

Vazquez-Duhalt, R. (1989). Environmental impact of used motor oil. *Sci. Total Environ.* 79 (1), 1–23. doi:10.1016/0048-9697(89)90049-1

Watkins, R. C. (1982). The antiwear mechanism of zddp's. Part II. *Tribol. Int.* 15 (1), 13–15. doi:10.1016/0301-679X(82)90102-5

Wilson, B. (1998). Lubricants and functional fluids from renewable sources. *Industrial Lubr. Tribol.* 50 (1), 6–15. doi:10.1108/00368799810781274

Yosief, H. O., Sarker, M. I., Bantchev, G. B., Dunn, R. O., and Cermak, S. C. (2022a). Physico-chemical and tribological properties of isopropyl-branched chicken fat. *Fuel* 316, 123293. doi:10.1016/j.fuel.2022.123293

Yosief, H. O., Sarker, M. I., Bantchev, G. B., Dunn, R. O., and Cermak, S. C. (2022b). Chemical modification of beef tallow for lubricant application. *Ind. Eng. Chem. Res.* 61 (27), 9889–9900. doi:10.1021/acs.iecr.2c01207

Zhang, J., and Spikes, H. (2016). On the mechanism of ZDDP antiwear film formation. *Tribol. Lett.* 63 (2), 24. doi:10.1007/s11249-016-0706-7

Zhang, Z., Li, Y., Luo, L., Yellezuome, D., Rahman, M. M., Zou, J., et al. (2023). Insight into kinetic and Thermodynamic Analysis methods for lignocellulosic biomass pyrolysis. *Renew. Energy* 202, 154–171. doi:10.1016/j.renene.2022.11.072